# Data-driven Iterative Learning Queuing Length Control Based on Vehicle-road Coordination Systems

**Biao Hong** * **Rui Wang** * **Xuhui Bu** *,**

* *School of Electrical Engineering and Automation, Henan Polytechnic University, Jiaozuo, China.*
** *Henan Key Laboratory of Intelligent Detection and Control of Coal Mine Equipment, Henan Polytechnic University, Jiaozuo, China.*
*(e-mail:hongbiao9598@163.com; wangrui12342022@126.com; Corresponding author e-mail: buxuhui@gmail.com)*

**Abstract:** Aiming at the intersection queuing length control, this paper establishes a model-free adaptive iterative learning control (MFAILC) scheme based on vehicle-road coordination systems. The MFAILC method is combined with the idea of vehicle speed guidance for the first time to deal with the traffic problem. Through the data communication between the vehicle and the road, a signal light control scheme is obtained, and then the vehicle guidance speed is given. The control objective is to make the queuing length at each intersection the shortest or the same. Firstly, the vehicle speed guidance scheme is given and the classical intersection model is analyzed. Since only controlling a single intersection does not play a great role in the traffic system, the research object of this paper is multi-intersection. Secondly, considering the complexity and repeatability of the intersection, its dynamic model is difficult to construct, so a MFAILC algorithm is presented. Then, the convergence of the proposed MFAILC scheme is derived. Finally, the feasibility of the MFAILC approach is verified by comparing the numerical simulation results.

*Keywords:* Intersection queuing length control, MFAILC, signal light control, vehicle-road coordination systems, vehicle speed guidance

## 1. INTRODUCTION

With the development of economy, more and more people own private cars. Whether it is for environmental protection or reducing the cost of everyone's travel, excellent intersection control plays an important role. Every year, a large number of urban road intersection control schemes are proposed. Despite this, intersection control is still one of the most challenging problems in the transportation system. The advent of computers is the dawn of solving traffic problems. In the 1950s, computers were first used to study traffic problems. Since the introduction of computers into the transportation system, the control of urban road intersection has become better. Robertson and Bretherton expounded the key principles of the real-time traffic signal optimizers in (Robertson and Bretherton, 1991). The method of controlling the signal sequences can reduce travel costs. Intelligent transportation system is one of the hottest research directions right now (Chalaki and Malikopoulos, 2022; Wang et al., 2022; Chen et al., 2022; Shu et al., 2022; Hwang and Choi, 2022; Karnati et al., 2022; Aoki and Rajkumar, 2022). Many valuable solutions have been proposed, both in road infrastructure and in control algorithms. The perfect roadside equipment (RSE) provides the possibility for the vehicle-road coordination system. In (Zhan et al., 2022), a hybrid allocation approach was developed for how to better deploy RSE on a highway. In (Xu et al., 2021), a non-signaled intersection management architecture that supports vehicle-road coordination is proposed. You et al. (You et el., 2015) addressed the tracking control problem for an autonomous lane change system. In (Lee and Park, 2012), a cooperative vehicle intersection control method was developed, which did not require a traffic signal. It can be found from the above description that the application of computer in the traffic system makes the intersection control more intelligent.

There are two types for intersection control: single intersection control and multi-intersection control. Generally, new methods are proposed for single intersection, and then applied to multi-intersection after continuous improvement. Guler et al. (Guler et el., 2014) discussed a method for improving the efficiency of intersections that utilized connected vehicle technology and was applicable to a single intersection. Hadjigeorgiou and Timotheou (Hadjigeorgiou and Timotheou, 2023) studied the application of connected and autonomous vehicles to reduce fuel consumption while driving safely. In (Hosseinzadeh et al., 2023), a multi-intersection control scheme based on model prediction was proposed, which was applied to emergency vehicle-centers. Hussain et al. (Hussain et al., 2022) developed a dynamic lighting system to help the driver react better at intersections. In (Wang et al., 2022), a traffic signal optimization method was developed to achieve uniform driving of vehicles at signalized intersections. Nevertheless,

the transportation system is still complex and difficult to model accurately. Considering the strong nonlinearity and periodicity of the intersection system, iterative learning control (ILC) and model-free adaptive control (MFAC) pop up in our minds.

In recent years, the ILC algorithm and the MFAC algorithm have been widely used in practical systems (Cobb et al., 2022; Yu et al., 2022; Xing et al., 2022; Wang et al., 2022; Li et al., 2023; Li and Hou, 2021; Lei et al., 2020; Shi et al., 2020; Liao et al., 2020). For repeatable systems, ILC has a very powerful control effect. In (Cobb et al., 2022), Cobb et al. discussed a path optimization algorithm based on iterative learning. Yu et al. (Yu et al., 2022) investigated the ILC problem based on neural networks. In (Boudjedir et al., 2021), Boudjedir et al. suggested a model-free ILC method applied to non-repetitive trajectories of robotic manipulators. Radac and Precup (Radac and Precup, 2015) proposed a concept of primitive-based ILC. Radac et al. (Radac et al., 2015) presented a model-free trajectory tracking of MIMO systems by the combination of ILC and primitives. MFAC is an excellent algorithm for complex systems that are difficult to build dynamic models. In (Li and Hou, 2021), Li and Hou proposed a hierarchical perimeter control mechanism for urban traffic networks based on MFAC algorithm. In (Lei et al., 2020), for the multi-region perimeter control problem, a MFAC method was proposed. Shi et al. (Shi et al., 2020) proposed a MFAC method to suppress the oscillation between wind farm areas. In (Liao et al., 2020), Liao et al. discussed the heading control problem of unmanned surface vehicles based on MFAC. Combining the characteristics of ILC and MFAC, Chi and Hou (Chi and Hou, 2007) proposed model-free adaptive ILC (MFAILC), which can be applied to the control problems of a large class of unknown nonlinear non-affine systems that operate repeatedly. MFAILC is suitable for many practical systems. In (Ren et al., 2021), a MFAILC algorithm for achieving precision control of the batch process was introduced. A distributed MFAILC method was proposed to deal the tracking problem (Bu et al., 2019). Ai et al. (Ai et al., 2020) presented a high-order pseudo partial derivative-based MFAILC approach. Yu et al. (Yu et al., 2022) discussed the application of MFAILC in trajectory tracking of wheeled mobile robots. Although MFAILC has been applied to many practical systems, there are still some systems suitable for MFAILC that have not been designed with corresponding control schemes.

Consequently, in this paper, an intersection control scheme based on the vehicle-road coordination system by employing the MFAILC mechanism is designed. The control scheme is divided into the following steps: firstly, the data information of vehicles and signal lights is obtained; then, the data is processed by using the MFAILC algorithm; finally, the reasonable signal light time and vehicle speed guidance information are given. Additionally, compared with the existing intersection control based on the vehicle-road coordination system, the contributions of this paper are as follows.

(a) The MFAILC scheme based on the vehicle-road coordination system is proposed for the first time to balance the queuing length at intersections, and the control objective is that the queuing length at each intersection is the shortest or the same.
(b) The control scheme proposed in this paper is a data-driven approach. The controller design and analysis use the I/O information of the system and do not rely on the multi-intersection model information. In addition, the MFAILC scheme does not need to design a controller for a certain process, that is, it can realize parameter adaptive control and structure adaptive control of nonlinear systems.
(c) In this paper, a reasonable vehicle speed guidance scheme is proposed, which provides the possibility for the application of the MFAILC algorithm in vehicle speed guidance.

The distribution of 2 to 5 sections is as follows. Problem formulation and algorithm design are given in Section 2. The convergence conditions of the MFAILC algorithm are analyzed in Section 3. Section 4 presents a simulation object, and Section 5 shows some conclusions.

## 2. PROBLEM FORMULATION AND ALGORITHM DESIGN

In order to better present the work of this paper, this section is divided into four subsections: vehicle speed guidance design, multi-intersection model, system descriptions and MFAILC algorithm design.

### *2.1 Vehicle speed guidance design*

When the classic signal control scheme is adopted at the intersection, the traffic conditions of vehicles are related to the time distribution of vehicles arriving at the intersection, and also related to the green light phase time of the intersection. This control is simple but not excellent. Therefore, this paper considers the vehicle speed guidance control method. The purpose of the vehicle speed guidance is to make the vehicle stop less or not stop when passing the intersection. The perfect speed guidance strategy is divided into the following types:

(1) When the driver drives to the intersection at a normal rate, if the current phase is passable and there are no queued vehicles ahead, he can pass immediately. In this case, increasing the speed of the vehicle can improve the efficiency of green light time utilization and reduce vehicle delays.
(2) When the driver drives to the intersection at a normal rate, if the current phase is passable and there are queued vehicles ahead, the vehicle should be induced according to the actual situation. (a) When there are fewer vehicles in the queue and the green light time is sufficient, the vehicle should be guided to slow down and follow the vehicle in front to pass the intersection quickly; (b) When there are many vehicles in the queue and the green light time is sufficient, the vehicle should be guided to drive at a lower speed and arrive at the intersection without stopping; (c) When there are many vehicles in the queue and the green light time is insufficient, the vehicle should be guided to travel at the lowest speed without stopping and to pass the intersection when the next green light comes on.

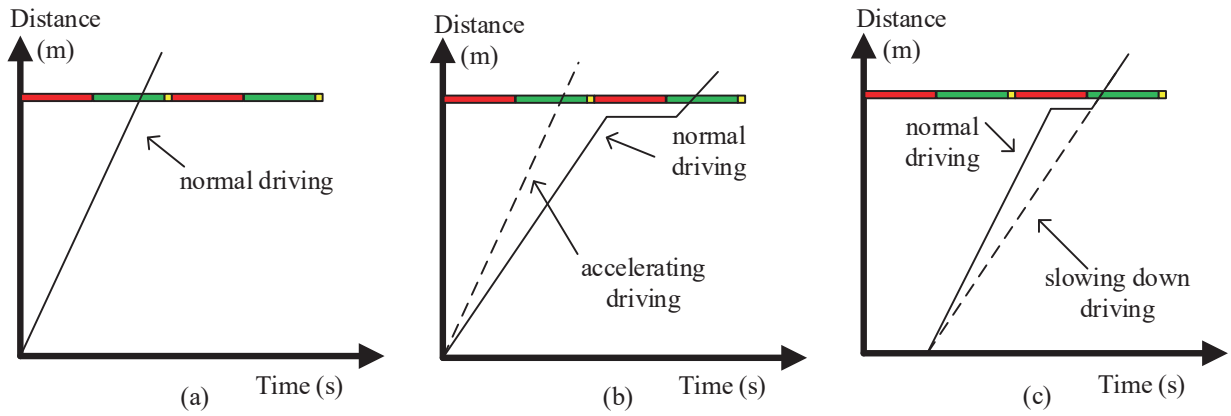


Fig. 1. Vehicle traffic status.

(3) When the driver drives to the intersection at a normal speed, if the current phase is the red light phase, the vehicle should be guide to slow down so that the vehicle can pass the intersection without stopping.

To apply the vehicle-road coordination system to the intersection control, the following conditions must be satisfied: Within the traffic area that needs to be processed, each intersection has a well-established infrastructure for data interaction with vehicles; all vehicles entering the road network have installed communication equipment and are networked; the communication performance between vehicles and road facilities is perfect without any packet loss and data transmission delay; the driver can adjust the vehicle speed in time according to the vehicle guidance speed. In addition, non-motorized vehicles and pedestrians are not considered, and traffic accidents are ignored.

This paper combines MFAILC with vehicle-road coordination for the first time to deal with the queuing length problem at intersections. A simpler guidance scheme is designed to verify the feasibility of the MFAILC method. The simpler guidance scheme is shown in Figure 1. As shown in Figure 1(a), when the driver drives to the intersection at a normal rate $v_{\text{free}}$, if the current phase is passable, there is no need to change the driving speed at this time.As shown in Figure 1(b), the current phase is impassable when the driver drives to the intersection at a normal rate, if the vehicle can accelerate to the intersection before the end of the last green light phase, the vehicle should drive at a higher speed $v_{\max}$. Figure 1(c) shows that the current phase is impassable when the driver drives to the intersection at a normal speed, if the vehicle cannot accelerate to the intersection before the end of the last green light phase, the vehicle should drive at a very low speed $v_{\min}$. The vehicle drives at the speed $v_{\min}$, which not only keeps the vehicle from stopping, but also enables the vehicle to pass at the next green light phase.

### *2.2 Multi-intersection model*

Single intersection control has limited ability to relieve traffic pressure in global road network control, while multi-intersection control can handle traffic problems well. Consequently, the research object of this paper is multi-intersection.

Because each intersection in the multi-intersection is a typical four-phase intersection, in order to better analyze the multi-intersection model, first a typical four-phase single intersection $A$ is build as shown in Figure 2. The intersection is divided into four directions: east, west, north and south. In each direction, only the straight signal and the left turn signal are considered, and the right turn signal is always green. The intersection is divided into four phases: phase 1 is east-west straight, phase 2 is east-west turn left, phase 3 is north-south straight, and phase 4 is north-south left turn. For the convenience of calculation, in the same phase at the same intersection, the larger queuing length is taken as the queuing length of the phase.

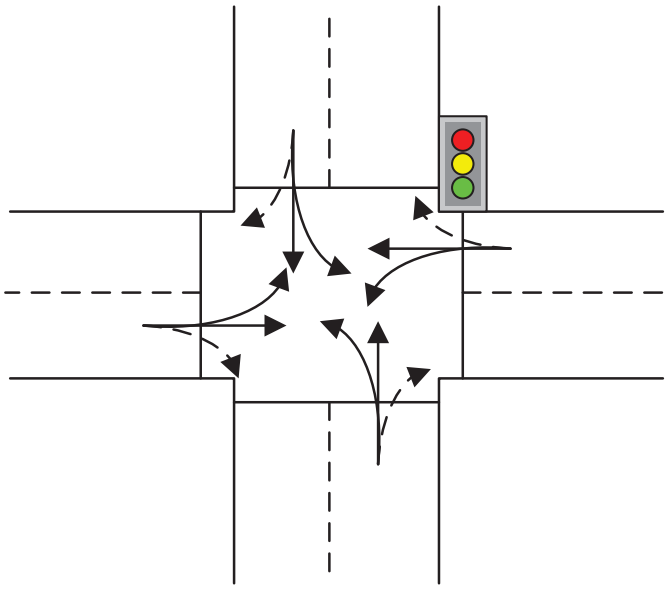

Fig. 2. Schematic diagram of a four-phase single intersection.

The queuing length of each phase at intersection $A$ is defined as

$$y_{Al}(k+1) = y_{Al}(k) + q_{Al}^{\text{in}}(k) - q_{Al}^{\text{out}}(k), \tag{1}$$

where $q_{Al}^{\text{in}}(k)$ and $q_{Al}^{\text{out}}(k)$ denote the inflow and outflow vehicle lengths of each phase at time instant $k$, and $l = \{1, 2, 3, 4\}$ is the phase. $q_{Al}^{\text{in}}(k)$ and $q_{Al}^{\text{out}}(k)$ are represented as

$$\begin{cases} q_{Al}^{\text{in}}(k) = Td_A(k) \\ q_{Al}^{\text{out}}(k) = Tv_{Al}(k), \end{cases} \tag{2}$$

where $T$ represents the cycle duration, $d_A(k)$ represents the vehicle arrival rate at intersection $A$, and $v_{Al}(k)$ is the vehicle dissipation rate of phase $l$ at intersection $A$.

The value formula of $v_{Al}(k)$ is expressed as follows

$$v_{Al}(k) = s_A u_{Al}(k)/T, \tag{3}$$

where $s_A$ is the saturated flow rate at intersection $A$ and $u_{Al}(k)$ is the green light duration of phase $l$ at intersection $A$. Substituting (2) and (3) into (1), the queuing length can be rewritten as

$$y_{Al}(k+1) = y_{Al}(k) + Td_A(k) - s_A u_{Al}(k). \tag{4}$$

In order to meet the actual road control requirements, the following constraints are given

$$\begin{cases} \sum_{l=1}^{4} u_{Al}(k) = T - t \\ u_{\min} \le u_{Al}(k) \le u_{\max}, \end{cases} \tag{5}$$

where $u_{\min}$ and $u_{\max}$ indicate the minimum and maximum green light duration, and $t$ is the lost time. So far, the single intersection model analysis is completed. The next step is to build a multi-intersection model on the basis of intersection $A$.

As shown in Figure 3, the multi-intersection system has eight queuing lengths, which are respectively expressed as $y_{1,1}$, $y_{1,2}$, $y_{1,3}$, $y_{1,4}$, $y_{2,1}$, $y_{2,2}$, $y_{2,3}$, and $y_{2,4}$. $L_z$ is the length of the road segment $z$ between intersection I1 and intersection I2. Both intersection I1 and intersection I2 are typical four-phase intersections. Furthermore, the sum of all vehicle lengths in any direction on road segment $z$ is denoted as

$$X_z(k+1) = X_z(k) + q_z^{\text{in}}(k) - q_z^{\text{out}}(k) + D_z(k), \tag{6}$$

where $q_z^{\text{in}}(k)$ and $q_z^{\text{out}}(k)$ are the number of vehicles flowing into and leaving road segment $z$ at time instant $k$. $D_z(k)$ stands for interference error. $q_z^{\text{in}}(k)$ and $q_z^{\text{out}}(k)$ are denoted as

$$\begin{cases} q_z^{\text{in}}(k) = \sum_{\alpha m \in U} r_{\alpha m} s_{\alpha m} u_{\alpha m}(k) \\ q_z^{\text{out}}(k) = \sum_{\beta m \in V} r_{\beta m} s_{\beta} u_{\beta m}(k), \end{cases} \tag{7}$$

where $U = \{\alpha 1, \alpha 2, \alpha 3\}$ represents the set of three directions that enter the road segment $z$, $V = \{\beta 1, \beta 2, \beta 3\}$ is the set of three directions outgoing the road segment $z$, $r_{\alpha m}$ and $r_{\beta m}$ are the inflow steering ratio and the outflow steering ratio. In addition, $s_{\alpha m}$ and $s_{\beta}$ are defined as saturated flow rates into and out of the road segment, $u_{\alpha m}(k)$ and $u_{\beta m}(k)$ are the green light times upstream and downstream of the road segment. The constraint conditions satisfied by the green light are the same as formula (5). Substituting (7) into (6), the following equation can be obtained

$$\begin{aligned} X_z(k+1) = X_z(k) &+ \sum_{\alpha m \in U} r_{\alpha m} s_{\alpha m} u_{\alpha m}(k) \\ &- \sum_{\beta m \in V} r_{\beta m} s_{\beta} u_{\beta m}(k) + D_z(k). \end{aligned} \tag{8}$$

Make $\boldsymbol{r} = [\ r_{\alpha 1} s_{\alpha 1},\ r_{\alpha 2} s_{\alpha 2},\ r_{\alpha 3} s_{\alpha 3},\ -r_{\beta 1} s_{\beta},\ -r_{\beta 2} s_{\beta},\ -r_{\beta 3} s_{\beta}]$ and $\boldsymbol{u}(k) = [\ u_{\alpha 1}(k),\ u_{\alpha 2}(k),\ u_{\alpha 3}(k),\ u_{\beta 1}(k),\ u_{\beta 2}(k), u_{\beta 3}(k)]^{\mathsf{T}}$, where $\mathsf{T}$ is a transposition symbol. Then, it can be obtained

$$X_z(k+1) = X_z(k) + \boldsymbol{r}\boldsymbol{u}(k) + D_z(k). \tag{9}$$

The queuing length function at the end of road segment $z$ is as follows

$$y_z(k+1) = y_z(k) + q(k) - p(k), \tag{10}$$

where $p(k) = q_z^{\text{out}}(k)$ and $q(k)$ is

$$q(k) = \min\{\rho_z(k) v_z(k) n_z T, X_z(k) - y_z(k)\}, \tag{11}$$

where $n_z$ represents the number of lanes in the same direction of road segment $z$, $\rho_z(k)$ and $v_z(k)$ are the vehicle density and speed of road segment $z$ at the $k$th cycle. According to Figure 1, the vehicle guidance speed is designed as

$$v_z(k) = \begin{cases} v_{\text{free}}, & \text{if } u_1 < u_z(k) < u_{\max} \\ v_{\max}, & \text{if } u_2 < u_z(k) < u_1 \\ v_{\min}, & \text{if } u_{\min} < u_z(k) < u_2, \end{cases} \tag{12}$$

where $v_{\text{free}}$, $v_{\max}$, $v_{\min}$, $u_{\max}$, $u_{\min}$, $u_1$, and $u_2$ are constants. $\rho_z(k)$ in (11) is represented as follows:

$$\rho_z(k) = \frac{X_z(k) - y_z(k)}{n_z \left( L_z - \dfrac{y_z(k)}{n_z \rho_{\max}} \right)}, \tag{13}$$

where the constant $\rho_{\max}$ is the maximum vehicle density. Observing (10), (11), (12), and (13), the functional relationship between $y_z(k+1)$ and $X_z(k)$ can be expressed as

$$y_z(k+1) = y_z(k) + f(X_z(k), y_z(k)) - q_z^{\text{out}}, \tag{14}$$

where $f(\cdot)$ is a nonlinear function. Let $\boldsymbol{b} = [0, 0, 0, -r_{\beta 1} s_{\beta}, -r_{\beta 2} s_{\beta}, -r_{\beta 3} s_{\beta}]$, equation (14) is transformed into

$$y_z(k+1) = y_z(k) + f(X_z(k), y_z(k)) - \boldsymbol{b}\boldsymbol{u}(k). \tag{15}$$

Combining (9) and (15), a multi-intersection queuing length system is obtained

$$\begin{cases} X(k+1) = X(k) + \boldsymbol{r}\boldsymbol{u}(k) + D(k) \\ y(k+1) = y(k) + f(X(k), y(k)) - \boldsymbol{b}\boldsymbol{u}(k). \end{cases} \tag{16}$$

Observing (16), it can be known that the queuing length $y(k+1)$ of vehicles is adjusted by controlling the green light duration $\boldsymbol{u}(k)$ in the multi-intersection system. In addition, it is worth noting that in view of the complexity of the actual road situation, this paper considers $D(k) = 0$.

In this paper, the maximum queuing length in all directions at the intersection is chosen as the queuing length at this intersection. Then, it can be obtained

$$\begin{cases} \mathfrak{L}_{\text{I1}}(k) = \max\ y_{\text{I1},l}(k), \quad l = 1, 2, 3, 4 \\ \mathfrak{L}_{\text{I2}}(k) = \max\ y_{\text{I2},l}(k), \quad l = 1, 2, 3, 4, \end{cases} \tag{17}$$

where $\mathfrak{L}_{\text{I1}}(k)$ and $\mathfrak{L}_{\text{I2}}(k)$ are the queuing lengths at intersection I1 and intersection I2, $y_{\text{I1},l}(k)$ and $y_{\text{I2},l}(k)$ are the queuing lengths for phase $l$ at time instant $k$ of intersection I1 and intersection I2. Besides, the queuing length difference (QLD) is proposed to reflect the effect of the control scheme. The formula of QLD is as follows

$$Y(k) = \mathfrak{L}_{\text{I1}}(k) - \mathfrak{L}_{\text{I2}}(k). \tag{18}$$

In this paper, the green light duration is selected as the control input and QLD is selected as the control output.

### *2.3 System descriptions*

Due to the nonlinear factors of practical intersections, this paper considers the following multiple input single output

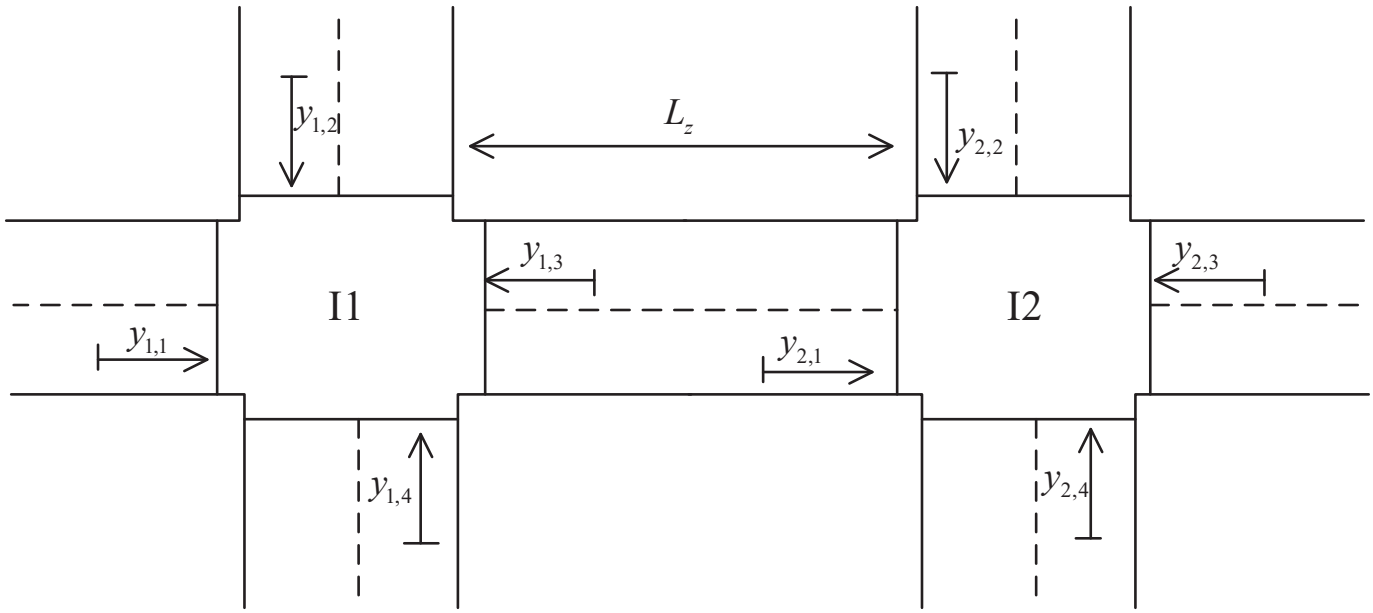


Fig. 3. Schematic diagram of four-phase multi-intersection.

discrete-time nonlinear systems to study the intersection control problem:

$$Y(k+1,i) = f(Y(k,i),\ldots,Y(k-n_Y,i), \boldsymbol{u}(k,i),\ldots,\boldsymbol{u}(k-n_u,i)), \quad (19)$$

where $Y(k,i)$ represents the QLD and is the system output, $\boldsymbol{u}(k,i) = [u_1(k,i), u_2(k,i),\ldots,u_8(k,i)]^{\mathsf{T}}$ represents the green light duration and is the control input, and $f(\cdot)$ is defined as an unknown nonlinear function. $k \in \{0,1,\ldots,N\}$ and $i = 1,2,\ldots$ are the time interval and the number of iterations, where $N$ denotes a finite positive integer. Besides, $n_Y$ is an unknown positive integer, and so is $n_u$.

Suppose the system (19) satisfies the following assumptions.

*Assumption 1.* The partial derivative of the function $f(\cdot)$ with respect to the $(n_Y+2)$th variable is continuous.

*Assumption 2.* The system (19) satisfies the generalized Lipschitz condition along the iterative axis, i.e., for all $k \in \{0,1,\ldots,N\}$ and $i = 1,2,\ldots$, if $\triangle \boldsymbol{u}(k,i) \neq 0$, the following formula holds

$$|\triangle Y(k+1,i)| \leq b\,||\,\triangle \boldsymbol{u}(k,i)\,|\,|, \quad (20)$$

where $\triangle Y(k+1,i) = Y(k+1,i) - Y(k+1,i-1)$, $\triangle \boldsymbol{u}(k,i) = \boldsymbol{u}(k,i) - \boldsymbol{u}(k,i-1)$, and $b$ is a positive constant.

*Remark 1.* For many control systems, Assumptions 1 and 2 are reasonable. In the design process of general nonlinear systems, Assumption 1 is always taken as the constraint condition. Assumption 2 is a restriction on the upper bound of the system output change rate. From the energy conversion point of view, the output energy change caused by a bounded input energy change should be bounded.

Satisfying the above two assumptions, the following theorem can be obtained.

*Theorem 1.* (Chi and Hou, 2007) The nonlinear system (19) satisfies the Assumptions 1 and 2, and when $\triangle u_\Upsilon(k,i) \neq 0, (\Upsilon = 1,2,\ldots,8)$, an iteration-related time-varying parameter $\boldsymbol{\Phi}(k,i)$ called the pseudo-partial derivative (PPD) can definitely be obtained. Meanwhile, $\boldsymbol{\Phi}(k,i)$ enables the system (19) to be transformed into a compact from dynamic linearization (CFDL) data model on the iterative axis, which can be represented as

$$\triangle Y(k+1,i) = \boldsymbol{\Phi}^{\mathsf{T}}(k,i)\ \triangle \boldsymbol{u}(k,i), \quad (21)$$

where $||\boldsymbol{\Phi}(k,i)|\,| < b$ for any time k and iteration i, and $\boldsymbol{\Phi}(k,i) = [\phi_1(k,i), \phi_2(k,i),\ldots,\phi_8(k,i)]^{\mathsf{T}}$.

**Proof.** See the proof of Theorem 1 in the work of (Chi and Hou, 2007) and (Hou and Jin, 2011).

*Remark 2.* $\boldsymbol{\Phi}(k,i)$ is essentially iteration-related time-varying parameter, which is related to the system input and output signals of the current $i$th iteration and the $i-1$th iteration to time $k$. $\boldsymbol{\Phi}(k,i)$ can also be regarded as a differential signal, and is bounded for any $i$ and $k$. When the value of $\triangle \boldsymbol{u}(k,i)$ is not very large, $\boldsymbol{\Phi}(k,i)$ can be regarded as time-varying parameters that iteratively change slowly. According to this property of $\boldsymbol{\Phi}(k,i)$, parameters estimator along the iterative axis can be designed to estimate it.

### *2.4 MFAILC algorithm design*

In the road network, some road segments are often crowded, and some road segments have few vehicles. This phenomenon reduces the utilization rate of the road and increases the travel cost for everyone. In order to solve this problem, a MFAILC scheme is developed.

Given the desired output $\mathfrak{D} = 0$ and let the tracking error be $e(k+1,i) = \mathfrak{D} - Y(k+1,i)$. The control goal is to find the suitable control input $\boldsymbol{u}(k,i)$ so that $e(k+1,i)$ converges to 0 when the number of iterations tends to infinity. The system (21) is rewritten as

$$Y(k+1,i) = Y(k+1,i-1) + \boldsymbol{\Phi}^{\mathsf{T}}(k,i)\ \triangle \boldsymbol{u}(k,i). \quad (22)$$

Considering the system (16), this article proposes the following MFAILC algorithm (Bu et al., 2019):

$$\hat{\boldsymbol{\Phi}}(k,i)=\hat{\boldsymbol{\Phi}}(k,i-1)+\frac{\eta\ \triangle\boldsymbol{u}(k,i-1)}{\mu+||\triangle\boldsymbol{u}(k,i-1)||^2}\times\big(\triangle Y(k+1,i-1)-\hat{\boldsymbol{\Phi}}^{\mathsf{T}}(k,i-1)\ \triangle\boldsymbol{u}(k,i-1)\big),\tag{23}$$

where $\hat{\boldsymbol{\Phi}}(k,i) = [\hat{\phi}_1(k,i),\hat{\phi}_2(k,i),\ldots,\hat{\phi}_8(k,i)]^{\mathsf{T}}$ is the estimated value of $\boldsymbol{\Phi}(k,i)$, $\eta>0$ is the step factor, and $\mu>0$ is a weighting factor.

$$\boldsymbol{u}(k,i)=\boldsymbol{u}(k,i-1)+\frac{\rho\hat{\boldsymbol{\Phi}}(k,i)}{\lambda+||\hat{\boldsymbol{\Phi}}(k,i)||^2}e(k+1,i-1),\tag{24}$$

where $\rho\in(0,1]$ is the step factor and $\lambda>0$ is a weighting factor.

$$\begin{aligned}\hat{\phi}_\Upsilon(k,i) =&\hat{\phi}_\Upsilon(k,1),\ \text{if}\ \left|\hat{\phi}_\Upsilon(k,i)\right|\le\varepsilon\\ &\text{or}\ |\ \triangle u_\Upsilon(k,i-1)|\le\varepsilon\\ &\text{or}\ \operatorname{sign}(\hat{\phi}_\Upsilon(k,i))\ne\operatorname{sign}(\hat{\phi}_\Upsilon(k,1)),\end{aligned}\tag{25}$$

where $\Upsilon=1,2,\ldots,8$, $\hat{\phi}_\Upsilon(k,1)$ represents the initial value of $\hat{\phi}_\Upsilon(k,i)$ and $\varepsilon$ represents a small positive constant.

*Remark 3.* The parameter iterative update algorithm (23), the learning control algorithm (24) and the parameter reset algorithm (25) make up the MFAILC algorithm. There are four adjustable parameters: $\mu$, $\lambda$, $\eta$ and $\rho$. The purpose of introducing the constants $\mu$, $\lambda$ into the algorithm is to prevent the divisor from being equal to zero. $\mu$ and $\lambda$ in algorithm (23) and (25) are penalty factors for the variation of $\hat{\boldsymbol{\Phi}}(k,i)$ and $\boldsymbol{u}(k,i)$. $\eta$ and $\rho$ are step-length factors, which are added to improve the generality of the control scheme (23)-(25). The choice of $\mu$, $\lambda$, $\eta$ and $\rho$ is that $\mu$, $\lambda$ satisfy $\mu,\lambda>0$, and $\eta$, $\rho$ satisfy $0<\eta,\rho\le1$. In addition, in the control process, it can be seen that the MFAILC scheme only uses the I/O data of the controlled system.

## 3. MAIN RESULTS

In this section, let the interference amount of the multi-intersection system be 0 and make the following assumptions.

*Assumption 3.* For all $k$ and $i$, the sign of $\Phi_\Upsilon(k,i)$ in the controlled system does not change, i.e., $\Phi_\Upsilon(k,i)>\kappa>0$, where $\kappa$ is a small positive number and $\Upsilon=1,2,\ldots,8$.

*Remark 4.* Assumption 3 expresses the meaning that the control direction is definite and invariable. For example, in this paper, the longer the green light time, the shorter the queue length. This is also a reasonable assumption for many practical systems.

*Theorem 2.* Consider that the multi-intersection system (16) satisfies Assumptions 1 to 3. For the MFAILC algorithm, a small positive number $\lambda_{\min}$ can definitely be found, such that when $\lambda>\lambda_{\min}$, the following conclusions are given: $\forall k\in\{0,1,\cdots,N\}$ and $\forall i=1,2,\cdots$, the estimated value $\hat{\Phi}_\Upsilon(k,i)$ of PPD is bounded; $\forall k\in\{0,1,\cdots,N\}$, the tracking error monotonically converges to 0 as the iteration $i$ tends to infinity, i.e., $\lim\limits_{i\to\infty}|e(k+1,i)|=0$.

**Proof.** The proof consists of two parts, the first is to prove the boundedness of $\hat{\boldsymbol{\Phi}}(k,i)$, and the second is to prove the convergence performance of the tracking error.

If $\left|\hat{\phi}_\Upsilon(k,i)\right|\le\varepsilon$ or $|\triangle\ \boldsymbol{u}_\Upsilon(k,i-1)|\le\varepsilon$ or $\operatorname{sign}(\hat{\phi}_\Upsilon(k,i))\ne\operatorname{sign}(\hat{\phi}_\Upsilon(k,1))$, then $\hat{\phi}_\Upsilon(k,i)$ is obviously bounded. For the other cases, the parameter estimation error is defined as

$$\mathfrak{E}(k,i)=\hat{\boldsymbol{\Phi}}(k,i)-\boldsymbol{\Phi}(k,i).\tag{26}$$

By subtracting $\boldsymbol{\Phi}(k,i)$ from both sides of equation (23), one obtains

$$\begin{aligned}\mathfrak{E}(k,i) =&\ \mathfrak{E}(k,i-1)-(\boldsymbol{\Phi}(k,i)-\boldsymbol{\Phi}(k,i-1))\\ &+\frac{\eta\ \triangle\boldsymbol{u}(k,i-1)}{\mu+||\ \triangle\boldsymbol{u}(k,i-1)||^2}\times\big(\triangle Y(k+1,i-1)\\ &-\hat{\boldsymbol{\Phi}}^{\mathsf{T}}(k,i-1)\ \triangle\boldsymbol{u}(k,i-1)\big).\end{aligned}\tag{27}$$

Let $\triangle\boldsymbol{\Phi}(k,i)=\boldsymbol{\Phi}(k,i)-\boldsymbol{\Phi}(k,i-1)$, and substituting (21) into (27), one obtains

$$\begin{aligned}\mathfrak{E}(k,i) =&\ \mathfrak{E}(k,i-1)-\triangle\boldsymbol{\Phi}(k,i)+\frac{\eta\ \triangle\boldsymbol{u}(k,i-1)}{\mu+||\ \triangle\boldsymbol{u}(k,i-1)||^2}\\ &\times\big(\boldsymbol{\Phi}^{\mathsf{T}}(k,i-1)\ \triangle\boldsymbol{u}(k,i-1)\\ &-\hat{\boldsymbol{\Phi}}^{\mathsf{T}}(k,i-1)\ \triangle\boldsymbol{u}(k,i-1)\big)\\ =&\ \mathfrak{E}(k,i-1)-\frac{\eta||\ \triangle\boldsymbol{u}(k,i-1)||^2}{\mu+||\ \triangle\boldsymbol{u}(k,i-1)||^2}\mathfrak{E}(k,i-1)\\ &-\triangle\boldsymbol{\Phi}(k,i)\\ =&\left(1-\frac{\eta||\ \triangle\boldsymbol{u}(k,i-1)||^2}{\mu+|\triangle\boldsymbol{u}(k,i-1)|^2}\right)\mathfrak{E}(k,i-1)-\triangle\boldsymbol{\Phi}(k,i).\end{aligned}\tag{28}$$

From equation (28), it can be observed when $0<\eta\le1$ and $\mu>0$, the function $\frac{\eta||\triangle\boldsymbol{u}(k,i-1)||^2}{\mu+||\triangle\boldsymbol{u}(k,i-1)||^2}$ is monotonically increasing with respect to $||\ \triangle\boldsymbol{u}(k,i-1)||^2$ and has a minimum value $\frac{\eta\varepsilon^2}{\mu+\varepsilon^2}$. So there is a positive constant $\theta$ that makes the following inequality true

$$0<\left|1-\frac{\eta||\ \triangle\ \boldsymbol{u}(k,i-1)||^2}{\mu+||\ \triangle\boldsymbol{u}(k,i-1)||^2}\right|\le1-\frac{\eta\varepsilon^2}{\mu+\varepsilon^2}=\theta<1.\tag{29}$$

From Theorem 1, it can be known that $||\boldsymbol{\Phi}(k,i)||$ has an upper bound $b$. Therefore, $||\boldsymbol{\Phi}(k,i)-\boldsymbol{\Phi}(k,i-1)||\le2b$ can be derived. Based on (28) and (29), it can be easily derived

$$\begin{aligned}||\mathfrak{E}(k,i)|| =&\left|1-\frac{\eta||\ \triangle\boldsymbol{u}(k,i-1)||^2}{\mu+||\ \triangle\boldsymbol{u}(k,i-1)||^2}\right|||\mathfrak{E}(k,i-1)||\\ &+||\ \triangle\boldsymbol{\Phi}(k,i)||\\ \le&\theta\,||\mathfrak{E}(k,i-1)||+2b\\ &\vdots\\ \le&\theta^{i-1}\,||\mathfrak{E}(k,1)||+\frac{2b}{1-\theta},\end{aligned}\tag{30}$$

so $\mathfrak{E}(k,i)$ is bounded. Furthermore, observing $||\boldsymbol{\Phi}(k,i)||\le b$ and (26), it can be obtained that $\forall k\in\{0,1,\cdots,N\}$ and $\forall i=1,2,\cdots$, $\hat{\boldsymbol{\Phi}}(k,i)$ is also bounded.

According to (21), the tracking error can be rewritten as

$$\begin{aligned}e(k+1,i) =&\mathfrak{D}-Y(k+1,i)\\ =&\mathfrak{D}-Y(k+1,i-1)-\boldsymbol{\Phi}(k,i)^{\mathsf{T}}\ \triangle\boldsymbol{u}(k,i)\\ =&e(k+1,i-1)-\boldsymbol{\Phi}^{\mathsf{T}}(k,i)\ \triangle\boldsymbol{u}(k,i).\end{aligned}\tag{31}$$

Substituting (24) into (31), it can be derived

$$e(k+1,i)=\left(1-\boldsymbol{\Phi}^{\mathsf{T}}(k,i)\frac{\rho\hat{\boldsymbol{\Phi}}(k,i)}{\lambda+||\hat{\boldsymbol{\Phi}}(k,i)||^2}\right)e(k+1,i-1).\tag{32}$$

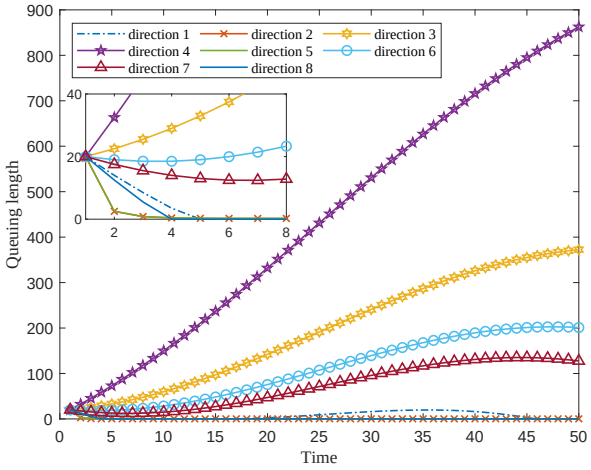


Fig. 4. Queuing lengths under the fixed allocation time.

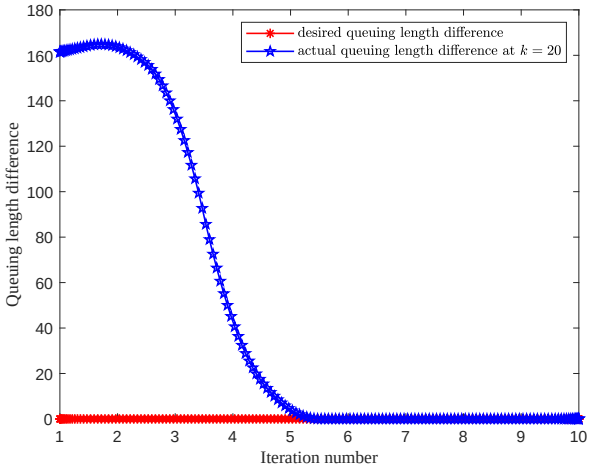


Fig. 5. Queuing length differences at $k = 20$.

Set $\lambda_{\min} = \frac{b^2}{4}$ and $\lambda > \lambda_{\min}$. In addition, according to the inequality $\mathbb{A}^2 + \mathbb{B}^2 \geq 2\mathbb{A}\mathbb{B}$, it can be known that there must be a constant $\mathfrak{R}$ $(0 < \mathfrak{R} < 1)$ to make the following formula true

$$\begin{aligned} 0 <& \mathfrak{R} \leq \frac{\boldsymbol{\Phi}^{\mathsf{T}}(k,i)\hat{\boldsymbol{\Phi}}(k,i)}{\lambda + ||\hat{\boldsymbol{\Phi}}(k,i)||^2} \leq \frac{b||\hat{\boldsymbol{\Phi}}(k,i)||}{\lambda + ||\hat{\boldsymbol{\Phi}}(k,i)||^2} \\ \leq& \frac{b||\hat{\boldsymbol{\Phi}}(k,i)||}{2\sqrt{\lambda}||\hat{\boldsymbol{\Phi}}(k,i)||} < \frac{b}{2\sqrt{\lambda_{\min}}} = 1. \end{aligned} \tag{33}$$

Utilizing formula (33), $\rho \in (0, 1]$, and $\lambda > \lambda_{\min}$, there must be a positive constant $\varphi$ $(\varphi < 1)$ such that the following formula holds

$$\begin{aligned} \left|1 - \frac{\rho\boldsymbol{\Phi}^{\mathsf{T}}(k,i)\hat{\boldsymbol{\Phi}}(k,i)}{\lambda + ||\hat{\boldsymbol{\Phi}}(k,i)||^2}\right| =& 1 - \frac{\rho\boldsymbol{\Phi}^{\mathsf{T}}(k,i)\hat{\boldsymbol{\Phi}}(k,i)}{\lambda + ||\hat{\boldsymbol{\Phi}}(k,i)||^2} \\ \leq& 1 - \rho\mathfrak{R} = \varphi < 1. \end{aligned} \tag{34}$$

Taking the absolute value of both sides of formula (32) and using (34), one obtains

$$\begin{aligned} |e(k+1,i)| =& \left|1 - \frac{\rho\boldsymbol{\Phi}^{\mathsf{T}}(k,i)\hat{\boldsymbol{\Phi}}(k,i)}{\lambda + ||\hat{\boldsymbol{\Phi}}(k,i)||^2}\right| |e(k+1,i-1)| \\ \leq& \varphi\,|e(k+1,i-1)| \leq \cdots \\ \leq& \varphi^{i-1}\,|e(k+1,1)|\,. \end{aligned} \tag{35}$$

Observing (35) and $\varphi < 1$, it is easy to conclude that $e(k+1,i)$ monotonically converges to 0 when the number of iterations $i$ tends to infinity. The proof is completed.

## 4. SIMULATION EXAMPLE

In order to verify the effectiveness of the proposed scheme, the simulation results of the system model Figure 3 are given and analyzed by comparison. This paper runs the simulation through the MATLAB R2021b software package. See subsections 2.1 and 2.2 for the realistic scenarios and control methods corresponding to the simulation. The simulation result under the fixed allocation time is shown in Figure 4, and the simulation results under the MFAILC scheme are shown in Figures 5–13. It is worth noting that all simulations in this section do not consider interference factors and are carried out under ideal conditions.

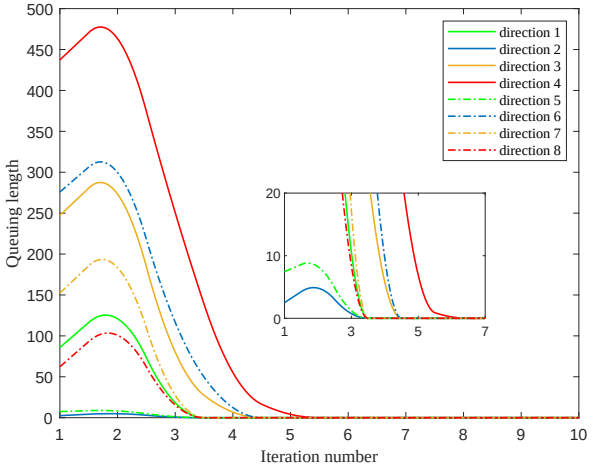


Fig. 6. Queuing lengths in all directions at $k = 20$.

The parameters used in this section are as follows. Given the desired output $\mathfrak{D} = 0$. The traffic flow entering the multi-intersection system is

$$\begin{aligned} X_1(k) &= 10 + 18\sin(k \times \pi/n) \\ X_2(k) &= 20 + 18\sin(k \times \pi/n) \\ X_3(k) &= 30 + 18\sin(k \times \pi/n) \\ X_4(k) &= 20 + 18\sin(k \times \pi/n) \\ X_5(k) &= 15 + 18\sin(k \times \pi/n) \\ X_6(k) &= 10 + 18\sin(k \times \pi/n), \end{aligned} \tag{36}$$

where $X_1(k), \ldots, X_6(k)$ are the traffic flows entering the multi-intersection system from six directions, respectively. Besides, $k \in \{1, 2, \ldots, 50\}$ and $n = 50$. The main parameters of the proposed MFAILC algorithm are chosen as $\eta = 1$, $\mu = 1$, $\rho = 0.2$, $\lambda = 0.01$, $\varepsilon = 10^{-5}$, and $\boldsymbol{\Phi}(1,1) = [0.1, 0.1, 0.1, 0.1, 0.1, 0.1, 0.1, 0.1]^{\mathsf{T}}$. The main parameters of the system (19) are selected as $s_1 = 0.55$, $s_2 = 0.6$, $L_z = 2000$m, $r_1 = \frac{1}{3}$, $r_2 = \frac{2}{3}$, and $\boldsymbol{u}(1,1) = 30$s.

The comparative experiment selected in this paper is the timing control scheme. Timing control is a more traditional method, that is, running the traffic signal controller

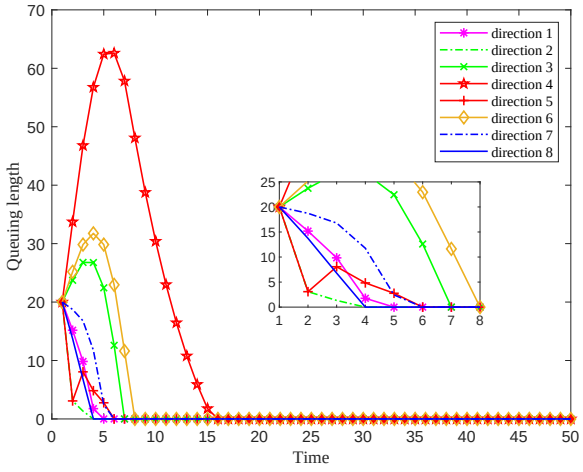


Fig. 7. Queuing lengths in all directions at the 5th iteration.

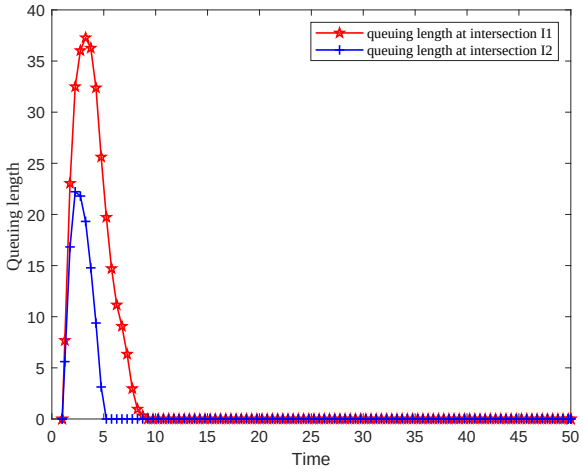


Fig. 8. Queuing lengths of two intersections at the 10th iteration.

according to the set timing scheme. The simulation model is exhibited in Figure 3, and the simulation results are shown in Figure 4. As shown in Figure 4, it can be clearly observed that some simulation curves of queuing lengths are divergent, and the distribution of queuing lengths in all directions is very uneven. In practice, this scheme can easily cause road congestion. Therefore, this paper proposes the MFAILC scheme to better deal with the traffic problem.

Figures. 5–13 are simulation results under the MFAILC scheme. Figure 5 shows the queuing length differences at $k = 20$. Queuing lengths in all directions at $k = 20$ are given in Figure 6. Obviously, when the iteration reaches 7, both the actual queuing length difference and the queuing lengths in all directions achieve very good results. Figure 7 shows the queuing lengths in all directions at the 5th iteration. It is observed from Figure 7 that all queuing lengths reach 0 before $k$ reaches 20. Figure 8 shows the queuing lengths of the two intersections at the 10th

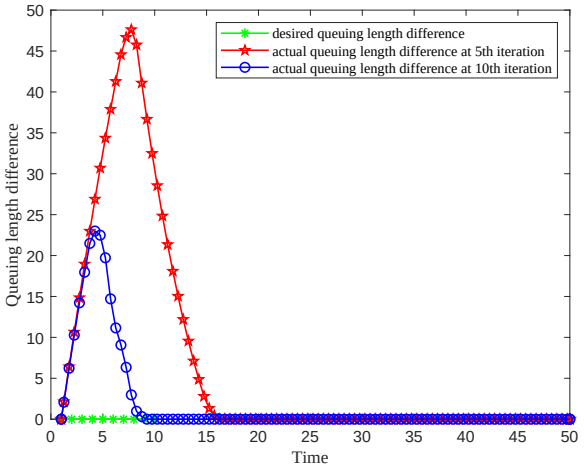


Fig. 9. Queuing length differences at the 5th and 10th iterations.

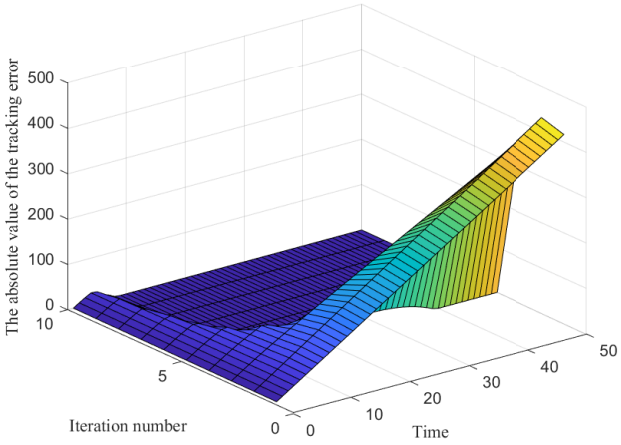


Fig. 10. The absolute value of the tracking error.

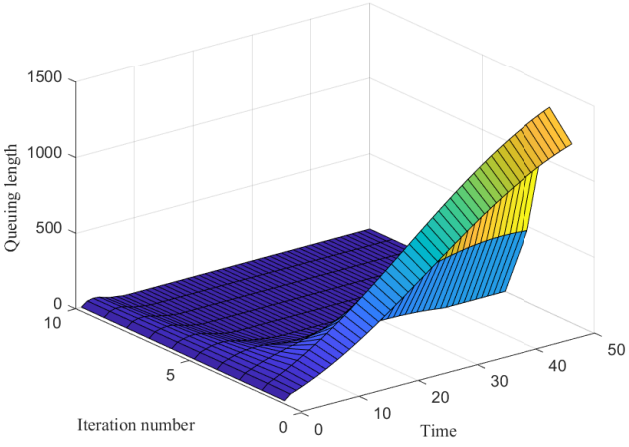


Fig. 11. Queuing length at intersection I1.

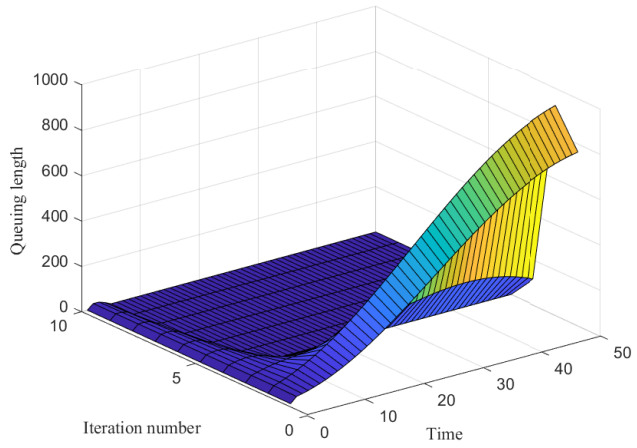


Fig. 12. Queuing length at intersection I2.

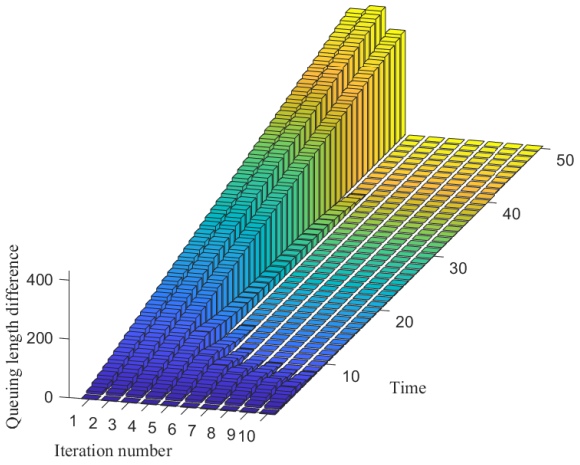


Fig. 13. Queuing length difference.

iteration. As shown in Figure 8, the queuing lengths of intersection I1 and intersection I2 have both converged to 0 when $k = 10$. Figure 9 shows the queuing length differences at the 5th and 10th iterations. It is observed from Figure 9 that the convergence rate at the 10th iteration is faster than that at the 5th iteration. Figure 10 presents the absolute value of the tracking error. It is observed from Figure 10 that the tracking error quickly converges to 0. Figures 11 and 12 show the queuing lengths at intersection I1 and intersection I2. The simulation result of the system output $Y(k, i)$ is shown in Figure 13. From Figures 11–13, it can be clearly observed that both the queuing lengths of the two intersections and the system output $Y(k, i)$ can converge to 0. The simulation results show that the MFAILC mechanism can not only make the queuing lengths of the two intersections the same but also make the queuing length in each direction the shortest. In conclusion, the effectiveness of the proposed MFAILC scheme is verified.

## 5. CONCLUSION

This paper proposes a MFAILC scheme for the multi-intersection queuing length control problem base on the vehicle-road coordination environment. Initially, a vehicle speed guidance scheme is designed, a multi-intersection model is built and linearized, and then a MFAILC mechanism is proposed. Moreover, the convergence performance of the MFAILC algorithm is discussed. After that, the simulation results verify the feasibility of the MFAILC scheme. The proposed MFAILC scheme helps to deal the problems of traffic congestion and uneven road utilization. In future research, we will consider how to make the proposed scheme feasible and effective in the presence of robustness issues.

## ACKNOWLEDGEMENTS

This work was supported in part by the National Natural Science Foundation of China under Grant U1804147, Grant 62273133 and Grant 61833001, and in part by the Innovative Scientists and Technicians Team of Henan Provincial High Education under Grant 20IRTSTHN019.

## REFERENCES

Ai Q, Ke D, Zuo J, et al. (2020). High-order model-free adaptive iterative learning control of pneumatic artificial muscle with enhanced convergence. *IEEE Transactions on Industrial Electronics* 67(11): 9548–9559.

Aoki S and Rajkumar R (2022). Cyber traffic light: safe cooperation for autonomous vehicles at dynamic intersections. *IEEE Transactions on Intelligent Transportation Systems* 23(11): 22519–22534.

Boudjedir CE, Bouri M and Boukhetala D. (2021). Model-free iterative learning control with nonrepetitive trajectories for second-order MIMO nonlinear systems-application to a delta robot. *IEEE Transactions on Industrial Electronics* 68(8): 7433–7443.

Bu X, Yu Q, Hou Z, et al. (2019). Model free adaptive iterative learning consensus tracking control for a class of nonlinear multiagent systems. *IEEE Transactions on Systems, Man, and Cybernetics: Systems* 49(4): 677–686.

Chalaki B and Malikopoulos AA (2022). Optimal control of connected and automated vehicles at multiple adjacent intersections. *IEEE Transactions on Control Systems Technology* 30(3): 972–984.

Chen C, Wu B, Xuan L, et al. (2022). A discrete control method for the unsignalized intersection based on cooperative grouping. *IEEE Transactions on Vehicular Technology* 71(1): 123–136.

Chi R and Hou Z (2007). Dual-stage optimal iterative learning control for nonlinear non-affine discrete-time systems. *Acta Automatica Sinica* 33(10): 1061–1065.

Cobb M, Reed J, Daniels J, et al. (2022). Iterative learning-based path optimization with application to marine hydrokinetic energy systems. *IEEE Transactions on Control Systems Technology* 30(2): 639–653.

Guler SI, Menendez M and Meier L (2014). Using connected vehicle technology to improve the efficiency of intersections. *Transportation Research Part C: Emerging Technologies* 46: 121–131.

Hadjigeorgiou A and Timotheou S (2023) Real-time optimization of fuel-consumption and travel-time of CAVs for cooperative intersection crossing. *IEEE Transactions on Intelligent Vehicles* 8(1): 313–329.

Hosseinzadeh M, Sinopoli B, Kolmanovsky I, et al. (2023). MPC-based emergency vehicle-centered multi-intersection traffic control. *IEEE Transactions on Control Systems Technology* 31(1): 166–178.

Hou Z and Jin S (2011). A Novel Data-Driven Control Approach for a Class of Discrete-Time Nonlinear Systems. *IEEE Transactions on Control Systems Technology* 19(6): 1549–1558.

Hussain Q, Alhajyaseen W, Brijs K, et al. (2022). Improved traffic flow efficiency during yellow interval at signalized intersections using a smart countdown system. *IEEE Transactions on Intelligent Transportation Systems* 23(3): 1959–1968.

Hwang Y and Choi SB (2022). Awareness on present and future trajectory of vehicle using multiple hypotheses in the mixed traffic of intersection. *IEEE Transactions on Intelligent Transportation Systems* 23(10): 17690–17703.

Karnati Y, Sengupta R, Rangarajan A, et al. (2022). Subcycle waveform modeling of traffic intersections using recurrent attention networks. *IEEE Transactions on Intelligent Transportation Systems* 23(3): 2538–2548.

Lee J and Park B (2012). Development and evaluation of a cooperative vehicle intersection control algorithm under the connected vehicles environment. *IEEE Transactions on Intelligent Transportation Systems* 13(1): 81–90.

Lei T, Hou Z and Ren Y (2020). Data-driven model free adaptive perimeter control for multi-region urban traffic networks with route choice. *IEEE Transactions on Intelligent Transportation Systems* 21(7): 2894–2905.

Liao Y, Jiang Q, Du T, et al. (2020). Redefined output model-free adaptive control method and unmanned surface vehicle heading control. *IEEE Journal of Oceanic Engineering* 45(3): 714–723.

Li D and Hou Z (2021). Perimeter control of urban traffic networks based on model-free adaptive control. *IEEE Transactions on Intelligent Transportation Systems* 22(10): 6460–6472.

Li J, You Z, Li Y, et al. (2023). Five-Axis contour error control based on spatial iterative learning. *IEEE Transactions on Automation Science and Engineering* 20(1): 112–123.

Radac MB and Precup RE. (2015). Optimal behaviour prediction using a primitive-based data-driven model-free iterative learning control approach. *Computers in Industry* 74: 95–109.

Radac MB, Precup RE and Petriu EM. (2015). Model-free primitive-based iterative learning control approach to trajectory tracking of MIMO systems with experimental validation. *IEEE Transactions on Neural Networks and Learning Systems* 26(11): 2925–2938.

Ren J, Liu D and Wan Y (2021). Model-free adaptive iterative learning control method for the czochralski silicon monocrystalline batch process. *IEEE Transactions on Semiconductor Manufacturing* 34(3): 398–407.

Robertson DI and Bretherton RD (1991). Optimizing networks of traffic signals in real time—the SCOOT method. *IEEE Transactions on Vehicular Technology* 40(1): 11–15.

Shi X, Cao Y, Shahidehpour M, et al. (2020). Data-driven wide-area model-free adaptive damping control with communication delays for wind farm. *IEEE Transactions on Smart Grid* 11(6): 5062–5071.

Shu H, Liu T, Mu X, et al. (2022). Driving tasks transfer using deep reinforcement learning for decision-making of autonomous vehicles in unsignalized intersection. *IEEE Transactions on Vehicular Technology* 71(1): 41–52.

Wang H, Patil SV, Aziz HMA, et al. (2022). Modeling and control using stochastic distribution control theory for intersection traffic flow. *IEEE Transactions on Intelligent Transportation Systems* 23(3): 1885–1898.

Wang J, Huang D, Fang S, et al. (2022). Model predictive control for ARC motors using extended state observer and iterative learning methods. *IEEE Transactions on Energy Conversion* 37(3): 2217–2226.

Wang Q, Zhou F, Xu J, et al. (2022). Tag-based verifiable delegated set intersection over outsourced private datasets. *IEEE Transactions on Cloud Computing* 10(2): 1201–1214.

Xing X, Xia J, Huang D, et al. (2022). Path learning in Human-Robot collaboration tasks using iterative learning methods. *IEEE Transactions on Control Systems Technology* 30(5): 1946–1959.

Xu Y, Zhou H, Ma T, et al. (2021). Leveraging multiagent learning for automated vehicles scheduling at nonsignalized intersections. *IEEE Internet of Things Journal* 8(14): 11427–11439.

You F, Zhang R, Lie G, et al. (2015). Trajectory planning and tracking control for autonomous lane change maneuver based on the cooperative vehicle infrastructure system. *Expert Systems with Applications* 42(14): 5932–5946.

Yu W, Wang R, Bu X, et al. (2022). Resilient model-free adaptive iterative learning control for nonlinear systems under periodic DoS attacks via a fading channel. *IEEE Transactions on Systems, Man, and Cybernetics: Systems* 52(7): 4117–4128.

Yu Y, Zhang C, Wang Y, et al. (2022). Neural-Network-Based iterative learning control for hysteresis in a magnetic shape memory alloy actuator. *IEEE/ASME Transactions on Mechatronics* 27(2): 928–939.

Zhan F, Jing P and Ran B (2022). Infrastructure allocation for improving sensing accuracy and connectivity probability based on combination strategy in vehicular networks. *IEEE Transactions on Intelligent Transportation Systems* 23(9): 15244–15255.